Supporting Information for Amplified Seasonal Range in Precipitation Minus Evaporation

Richard P. Allan

Department of Meteorology/National Centre for Earth Observation, University of Reading, Reading, Berkshire, UK

E-mail: r.p.allan@reading.ac.uk

July 5th 2023

The supporting information consists of additional supplementary figures and text.

1. Extended Method

Initial investigations of the global mean time series of P and E showed systematic biases between datasets but also drifts over time. Additionally the observations and reanalysis estimates do not represent a globally balanced water cycle, such that global mean P-E $\neq 0$, after accounting for the small atmospheric moisture storage change (Fig. S1). To ensure physical consistency, adjustments were applied to each observations-based dataset combination to ensure global annual mean $P - E = 0$. Based on assessment of the global mean timeseries (Fig. S1a) it was decided to apply an adjustment to evaporation based on the larger drifts over time compared to precipitation and since this field is not well observed compared to precipitation. Further inspection suggested that a global correction would introduce biases in some regions where evaporation totals are low and particularly over land where unrealistic negative multiannual $P - E$ was generated in some regions. Therefore a global annual scaling factor δ_y was applied to ocean evaporation, such that the largest adjustment was applied in regions of greater evaporation:

$$\delta_y A_{ocean} \overline{E_{y\_ocean}} = (\overline{P_y} - \overline{E_y}); \qquad E'_{m,y\_ocean} = E_{m,y\_ocean}(1 + \delta_y) \tag{1}$$

where subscripts m and y denote month and year and overbars denote annual averages applied over the globe or global ocean and A_{ocean} is the ocean area as a fraction of the globe. Figure S2g-h illustrate the mean spatial pattern of the P-E adjustment for GPCP-ERA5 and ERA5 over the 1995-2014 period, the largest adjustment (negative in the case of the combined GPCP-ERA5 dataset and positive in the case of ERA5) applying to the ocean regions with largest evaporation.

Monthly mean data from the observational (filled and unfilled), reanalysis and climate models spanning 1950–2100 and depending on the data record lengths were processed using *cdo* software (version 1.9.5; http://mpimet.mpg.de/cdo). Datasets were bi-linearly interpolated onto a common 0.75×0.75 latitude-longitude grid. Monthly

global and tropical (30^{o}S-30^{o}N) means were computed over the land, ocean and all regions using a common land-sea mask derived from the reanalysis data (land is assumed if more than half of the interpolated grid points are land points).

2. Supporting Tables and Figures

Table S1: Global mean annual monthly maximum and minumum P-E, 1995-2014 (note that 2014 was excluded from the 3-month analysis in Table 2, explaining slight differences in the global land annual mean).

P-E (mm/day)	Global				Global Land					
	MAX		MIN		MEAN		MAX		MIN	
Model/experiment	hist	amip	hist	amip	hist	amip	hist	amip	hist	amip
ACCESS-ESM1-5	4.50	4.32	-2.79	-2.75	1.16	1.35	6.44	6.88	-1.70	-1.74
BCC-CSM2-MR	4.52	4.46	-2.69	-2.74	1.17	1.31	6.93	7.65	-1.19	-1.58
BCC-ESM1	4.36	4.29	-2.59	-2.6	1.46	1.25	7.66	7.25	-1.42	-1.48
CanESM5	4.12	3.94	-2.70	-2.66	0.97	1.15	6.83	7.33	-2.20	-2.23
CESM2	4.08	3.79	-2.70	-2.64	1.24	1.53	6.78	7.18	-1.70	-1.59
CESM2-WACCM	3.95	3.76	-2.66	-2.63	1.25	1.50	6.72	7.08	-1.68	-1.61
CMCC-CM2-SR5	3.81	3.53	-2.66	-2.62	1.21	1.44	5.90	6.18	-1.58	-1.45
CNRM-CM6-1	4.31	4.15	-2.94	-2.93	0.93	0.86	5.76	5.03	-1.88	-1.68
CNRM-ESM2-1	4.32	4.18	-2.98	-2.93	0.95	0.87	5.82	5.12	-1.90	-1.68
GFDL-ESM4	4.26	4.22	-2.74	-2.73	0.94	1.00	6.78	6.6	-2.11	-2.02
GISS-E2-1-G	4.29	4.38	-2.77	-2.80	0.66	0.54	4.94	4.75	-1.67	-1.68
HadGEM3-GC31-LL	4.41	4.41	-2.83	-2.86	0.93	0.87	5.54	5.18	-1.63	-1.58
INM-CM5-0	3.97	4.08	-2.64	-2.72	1.06	0.99	5.49	5.26	-1.57	-1.59
IPSL-CM6A-LR	4.15	3.96	-2.82	-2.77	1.38	1.62	6.10	6.24	-1.44	-1.28
MIROC6	4.21	4.44	-2.81	-2.9	1.14	0.96	6.97	6.24	-2.03	-1.90
MRI-ESM2-0	4.22	4.03	-2.85	-2.85	1.04	1.22	6.01	6.34	-2.00	-2.02
NorESM2-LM	3.98	3.87	-2.63	-2.66	0.95	1.21	6.23	6.44	-1.83	-1.81
UKESM1-0-LL	4.35	4.37	-2.83	-2.86	0.94	0.92	5.55	5.28	-1.71	-1.63
Ensemble mean	4.21	4.12	-2.76	-2.76	1.08	1.14	6.25	6.22	-1.74	-1.70
GPCP/ERA5-adj		3.91		-2.81		1.01		5.48		-1.54
ERA5-adj		3.67		-2.53		1.12		5.35		-1.35
ERA5-MDiv-adj		3.75		-2.59		1.08		5.49		-1.65

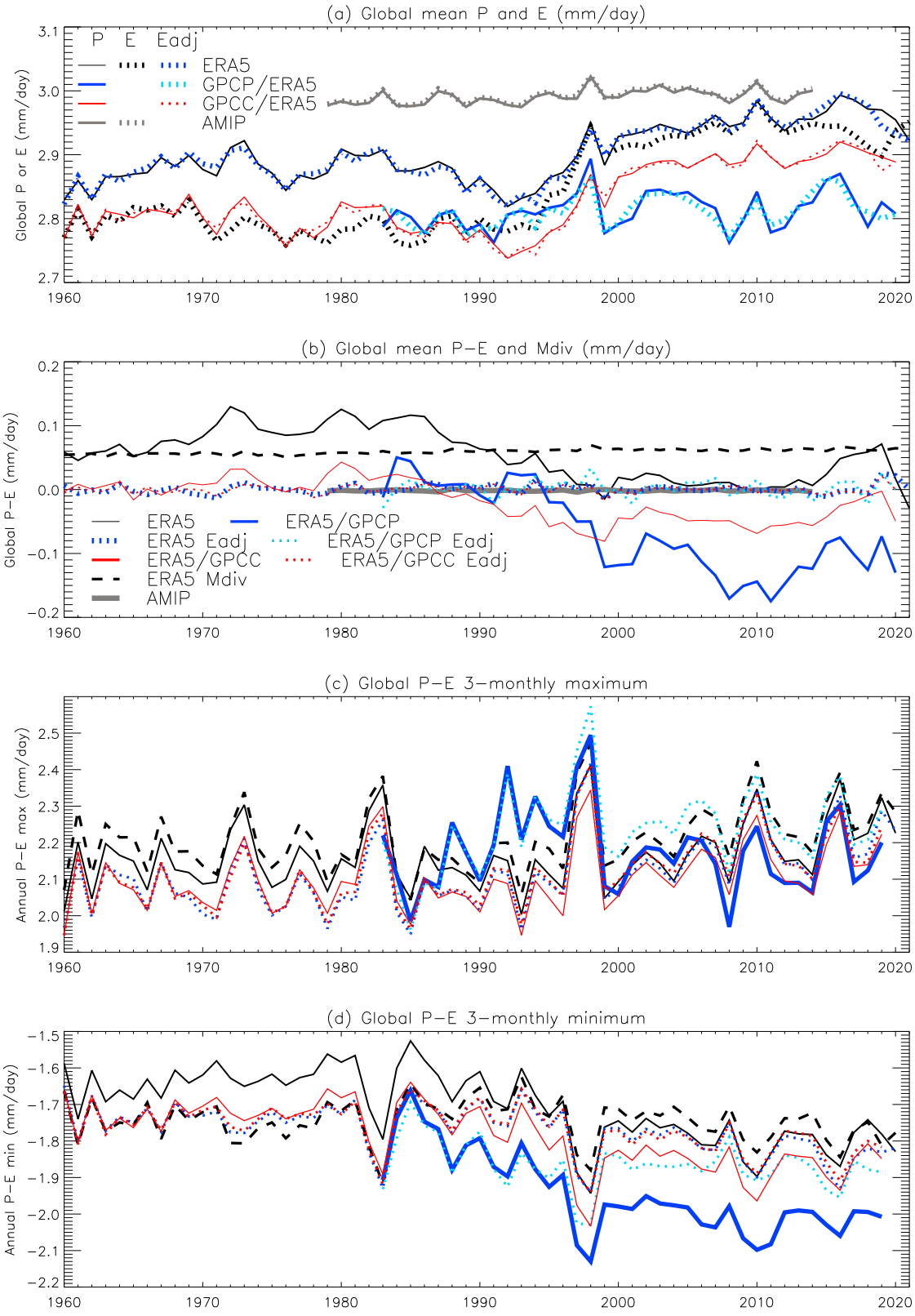

Figure S1: Global mean time series of (a) precipitation (P) and evaporation (E), (b) P−E and 3-month annual (c) maximum and (d) minimum P−E in a range of dataset combination. In (b-d), dotted lines denote ocean evaporation adjusted datasets such that global annual P−E = 0 (See Text S1).

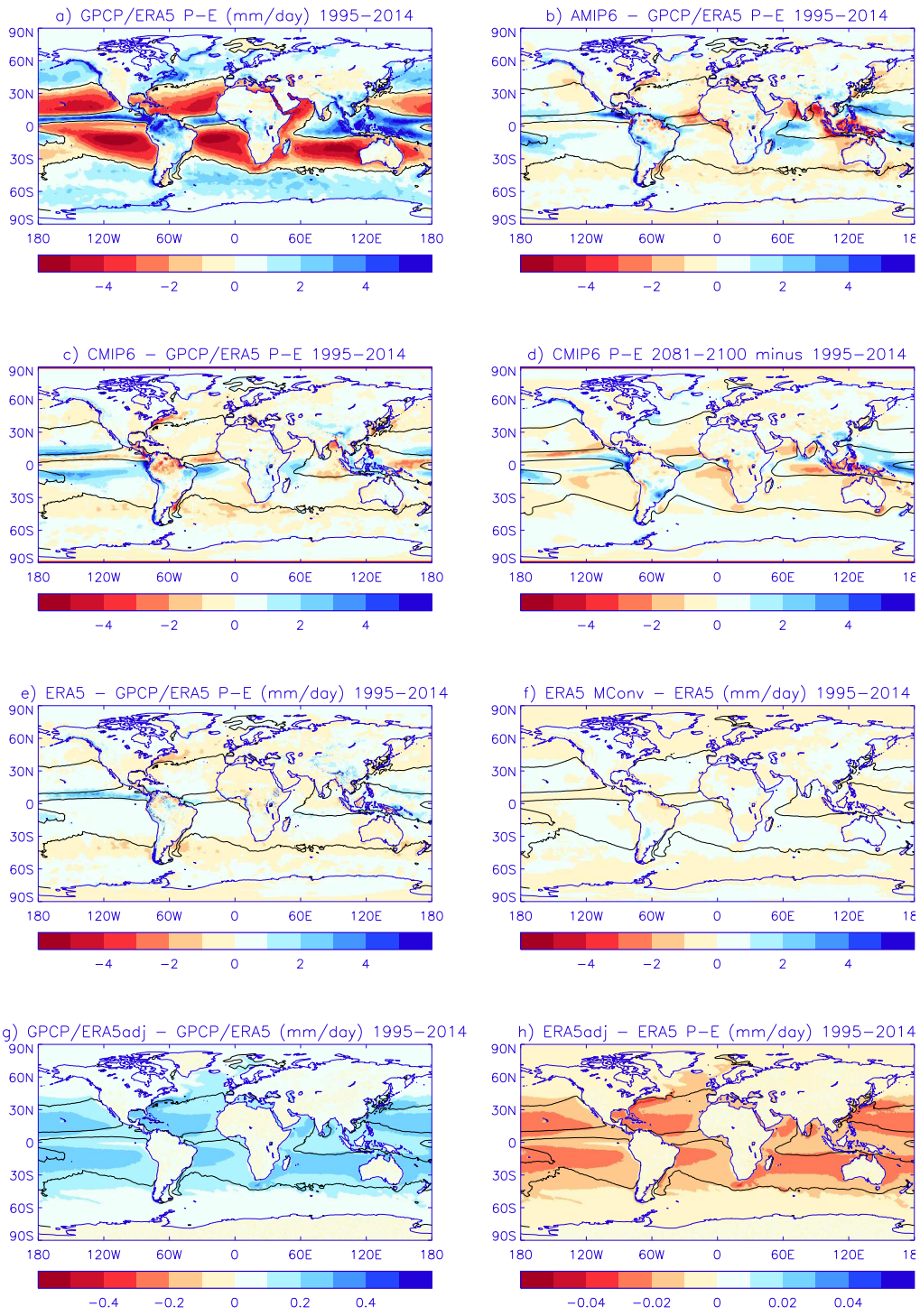

Figure S2: GPCP/ERA5 climatological P−E 1995-2014 (a) and P−E differences (1995-2014 relative to GPCP/ERA5 unless stated) for (b) CMIP6 *amip* multi-model mean, (c) CMIP6 *historical* multi-model mean, (d) CMIP6 *ssp2-4.5* 2081-2100 minus *historical* 1995-2014 projected multi-model mean change, (e) ERA5, (f) ERA5 moisture divergence estimate minus ERA5, and differences from evaporation adjustment to global P−E=0 for (g) GPCP/ERA5 and (h) ERA5.

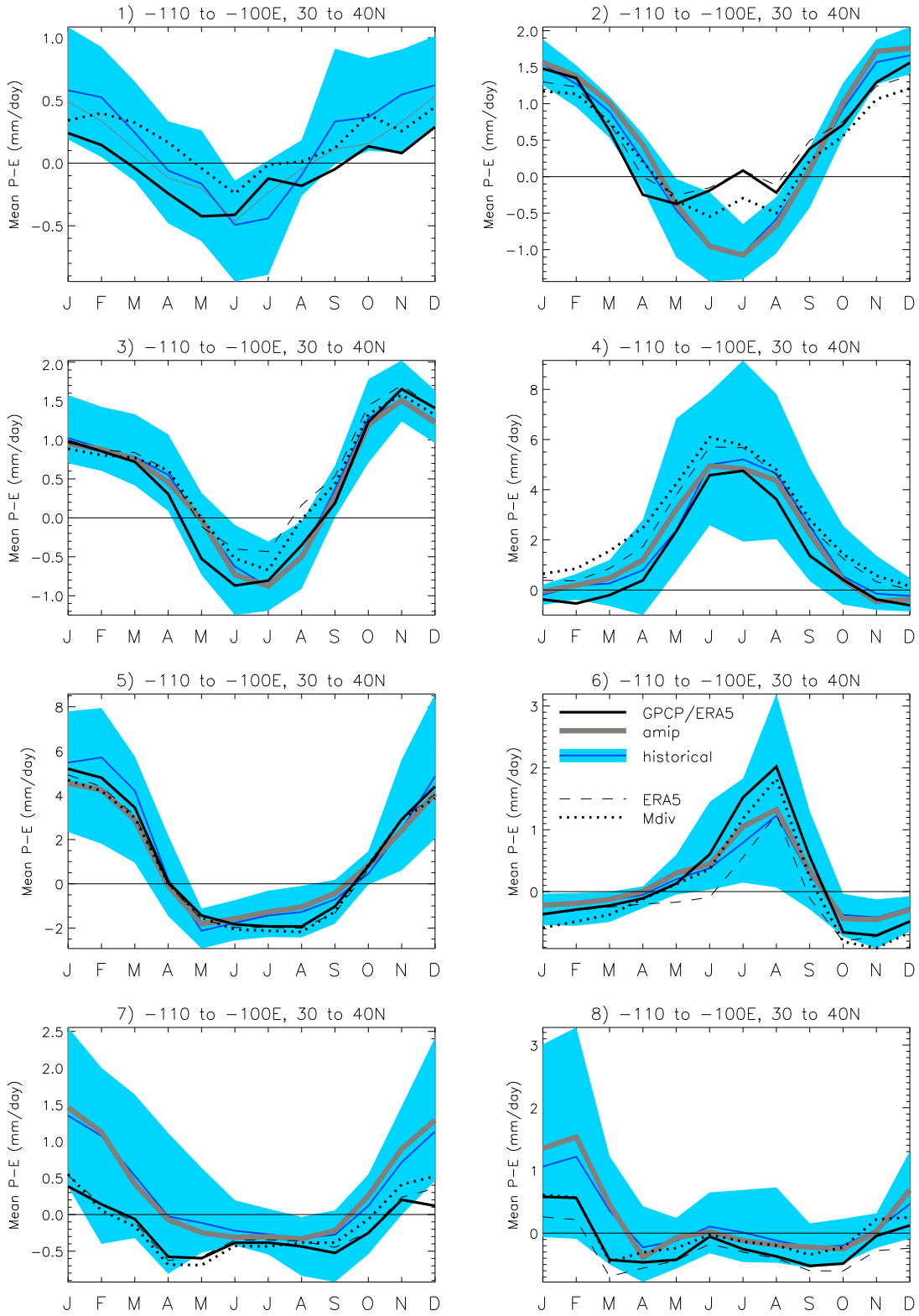

Figure S3: Seasonal cycles in P−E reproduced from Fig. 1 but also including *amip* multi-model mean estimates and ERA5.

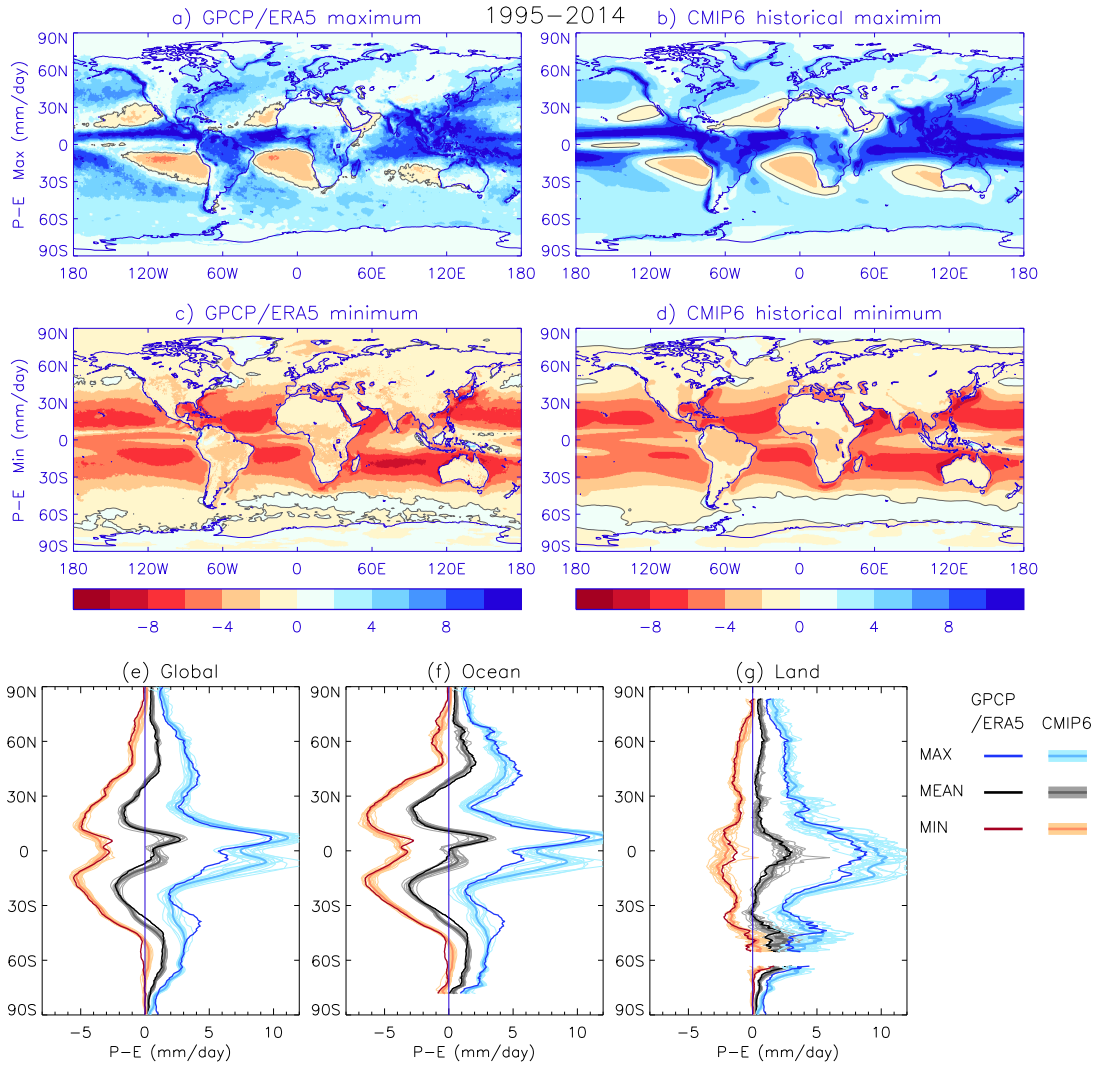

Figure S4: As Fig. 2 but for annual monthly maximum and minimum P−E and for 1995-2014.

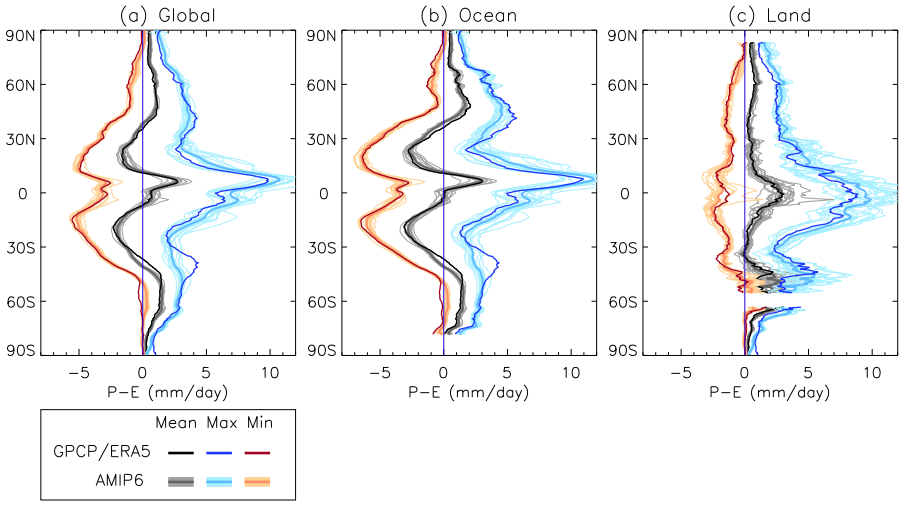

Figure S5: As Fig. S2e-f but for *amip* simulations.

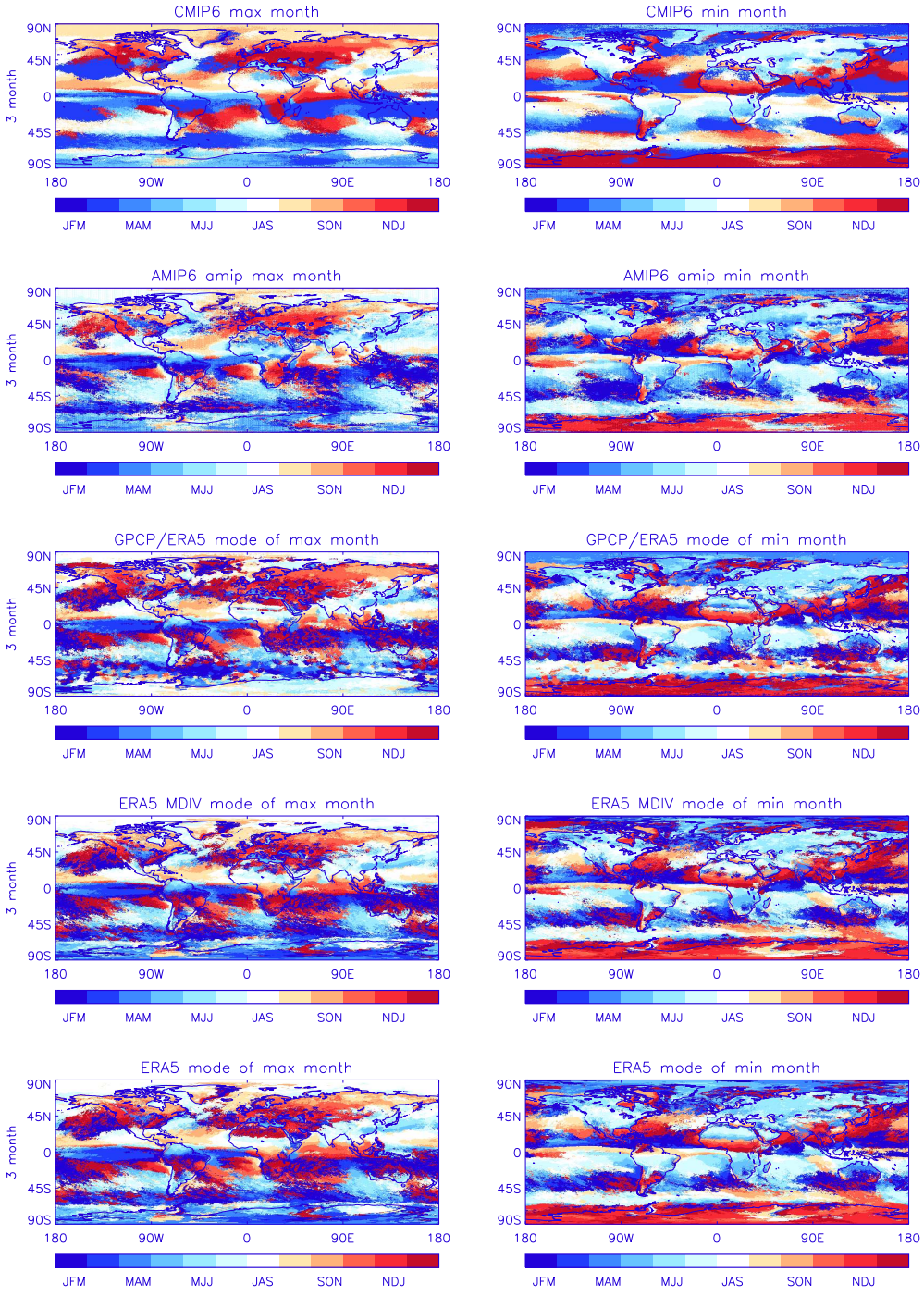

Figure S6: Modal seasonal timing of 3-month maximum (left) and minimum (right) in P-E (1995-2013) for CMIP6 *historical* multi-model mean, *amip* multi-model mean, GPCP/ERA5, ERA5 moisture divergence estimate and ERA5.

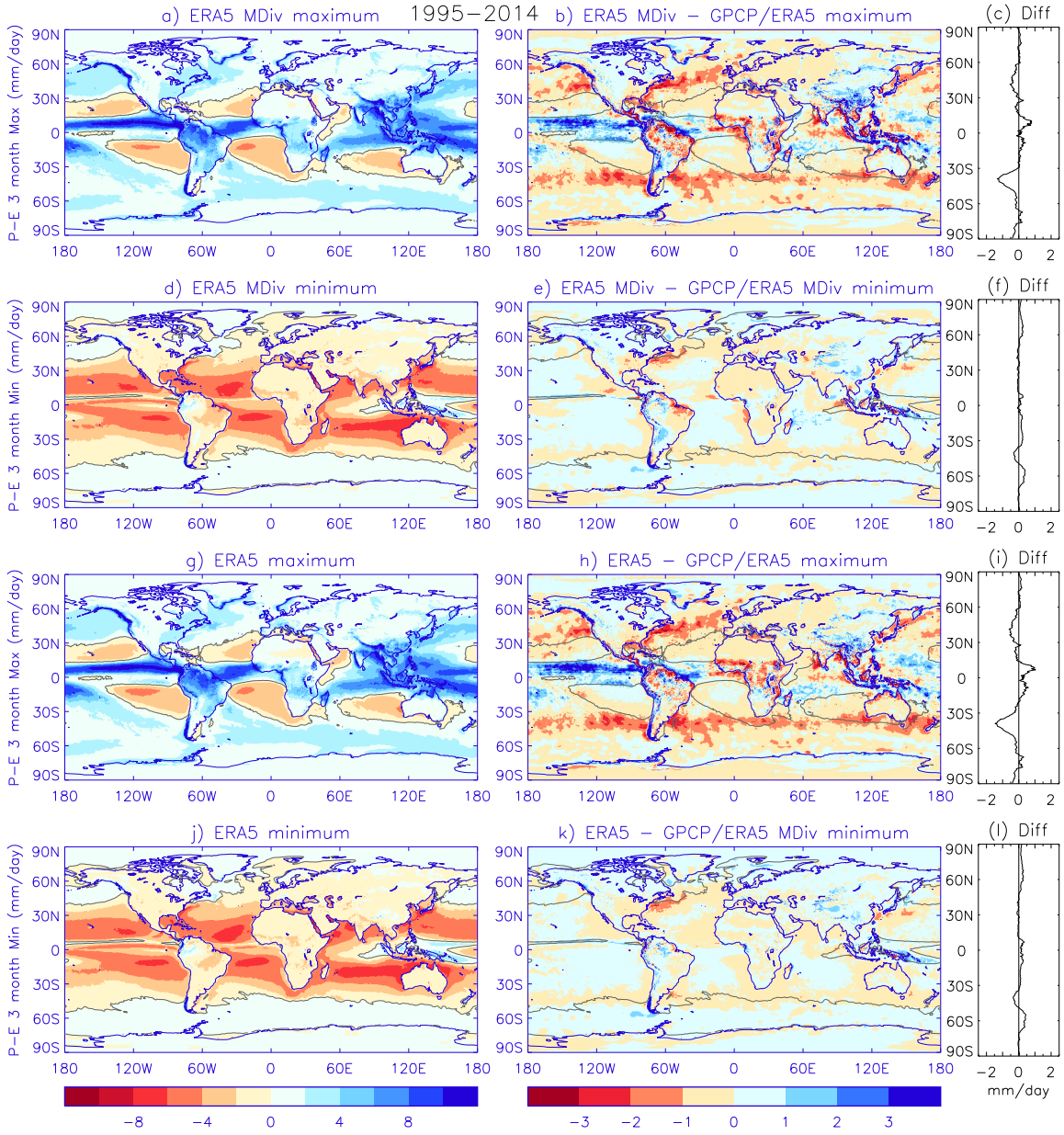

Figure S7: Mean annual 3-month maximum and minimum P−E and difference to GPCP/ERA5 for ERA5 moisture divergence (a-f) and ERA5 (g-l)

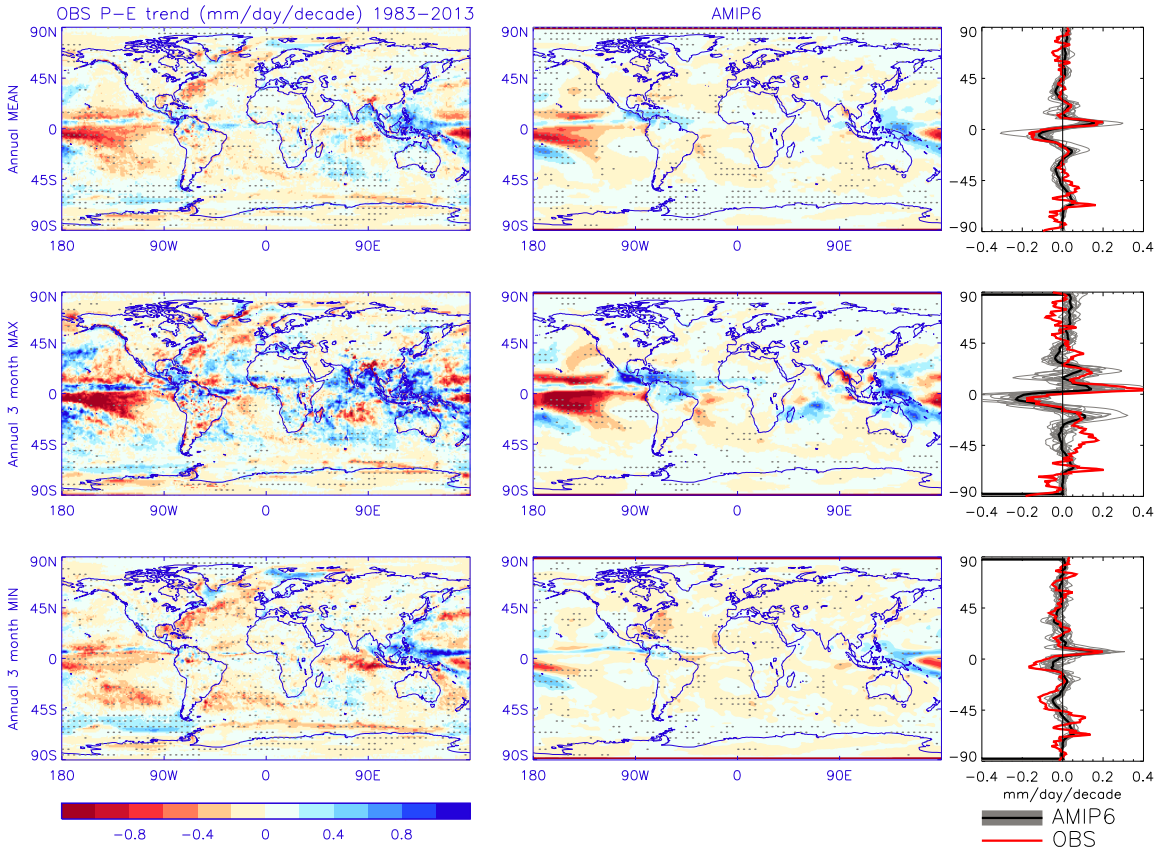

Figure S8: As Fig. 3 but for 1983-2013 trends in GPCP/ERA5 observations and *amip* multi-model mean P−E.

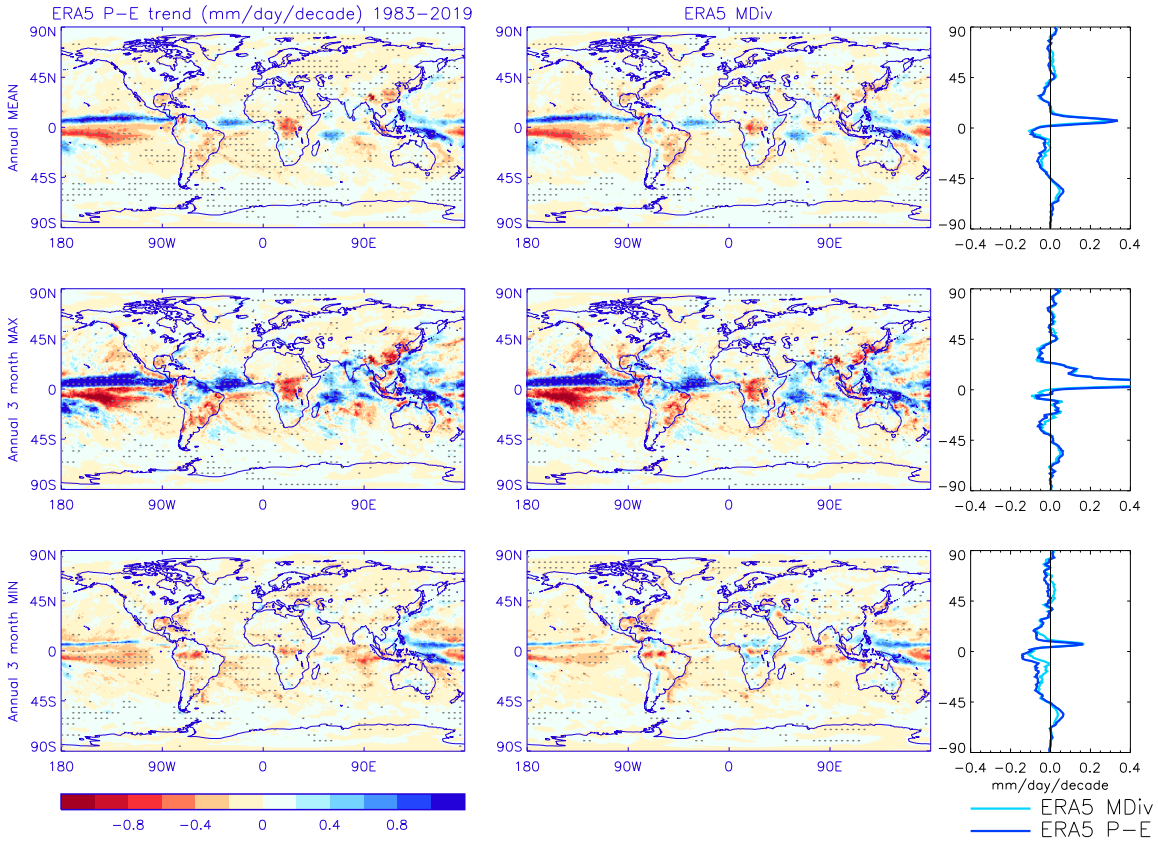

Figure S9: As Fig. 3 but for 1983-2019 trends in ERA5 and ERA5 moisture divergence P−E estimate.

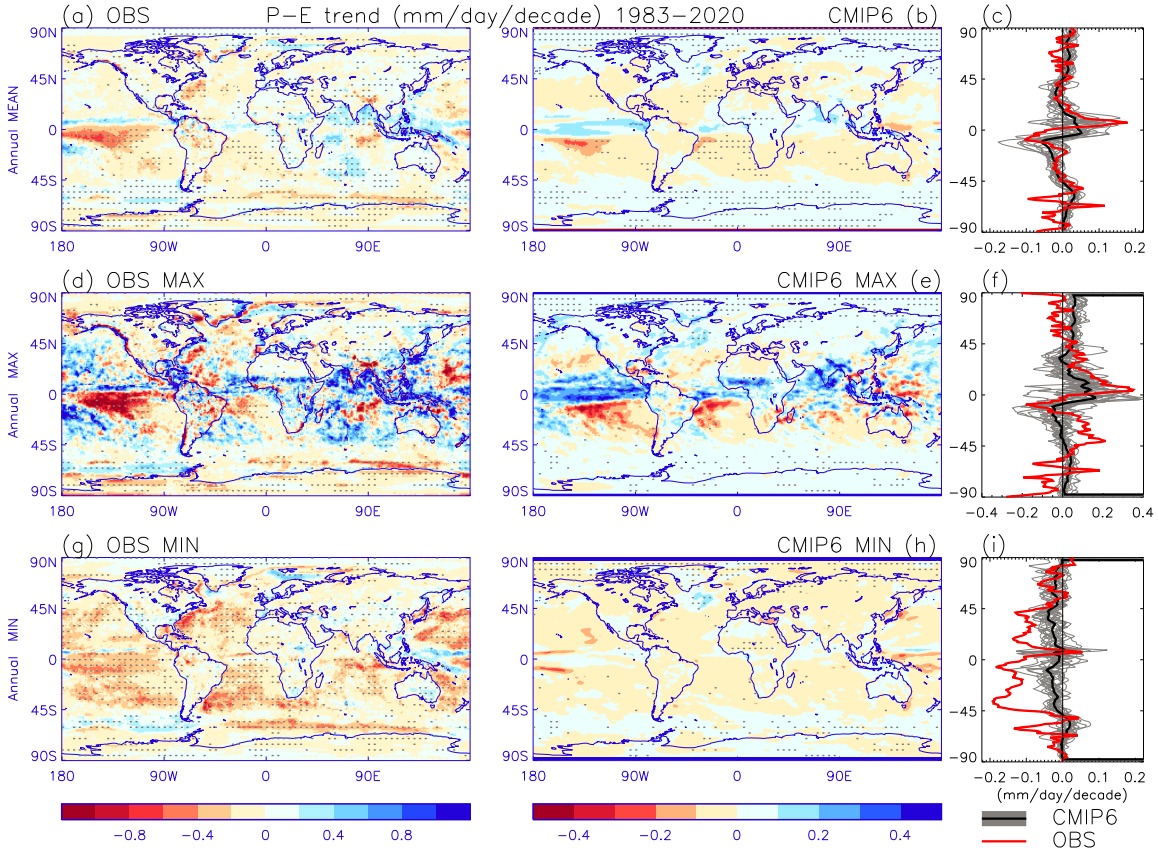

Figure S10: As Fig. 3 but for 1983-2020 trends in annual 1-month maximum P−E.

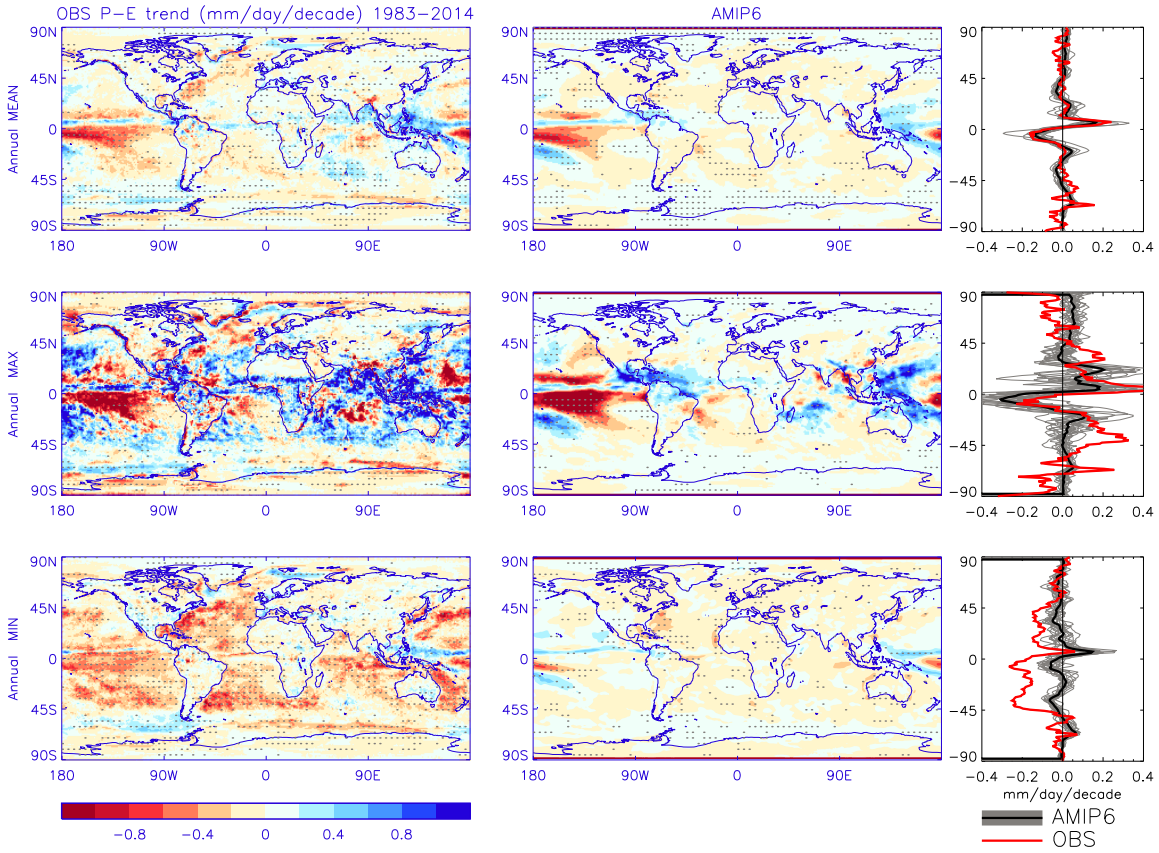

Figure S11: As Fig. 3 but for 1983-2020 trends in annual 1-month maximum for GPCP/ERA5 and *amip* multi-model mean P−E.

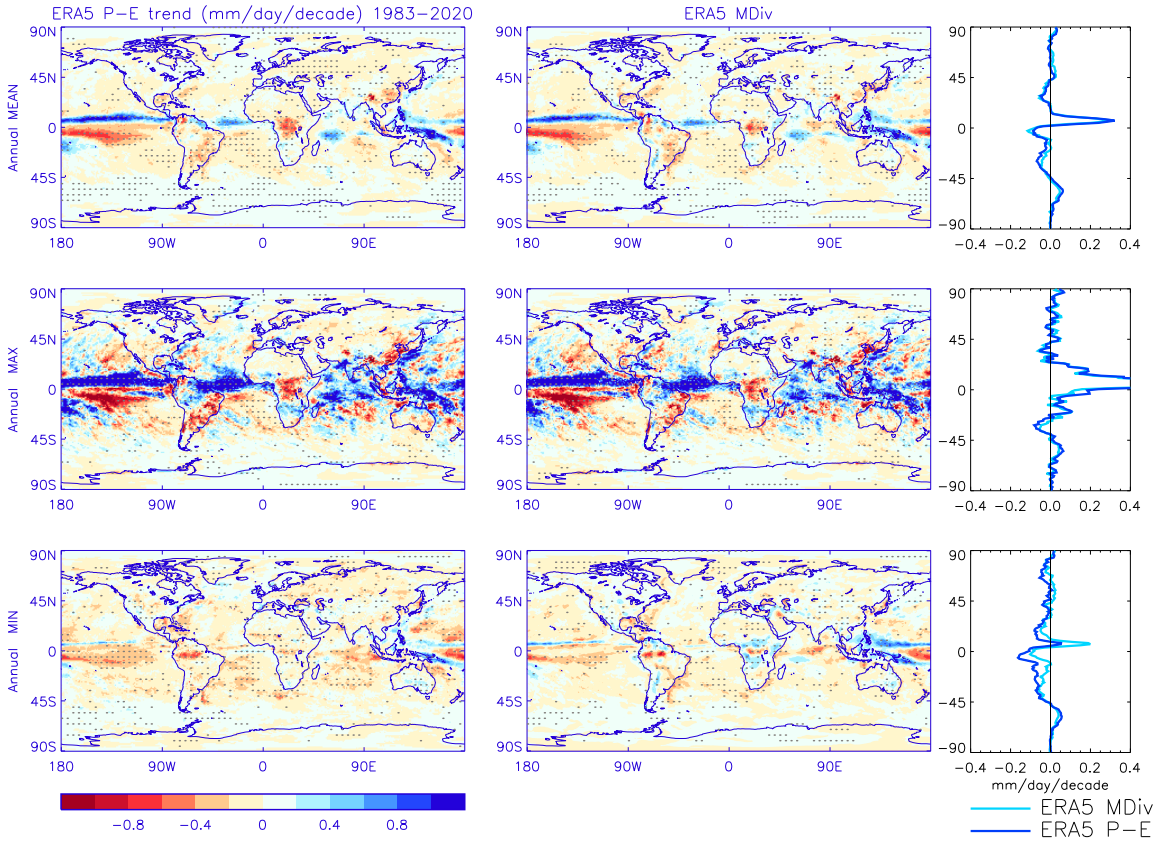

Figure S12: As Fig. 3 but for 1983-2020 trends in annual 1-month maximum for ERA5 and ERA5 moisture divergence P−E estimate.

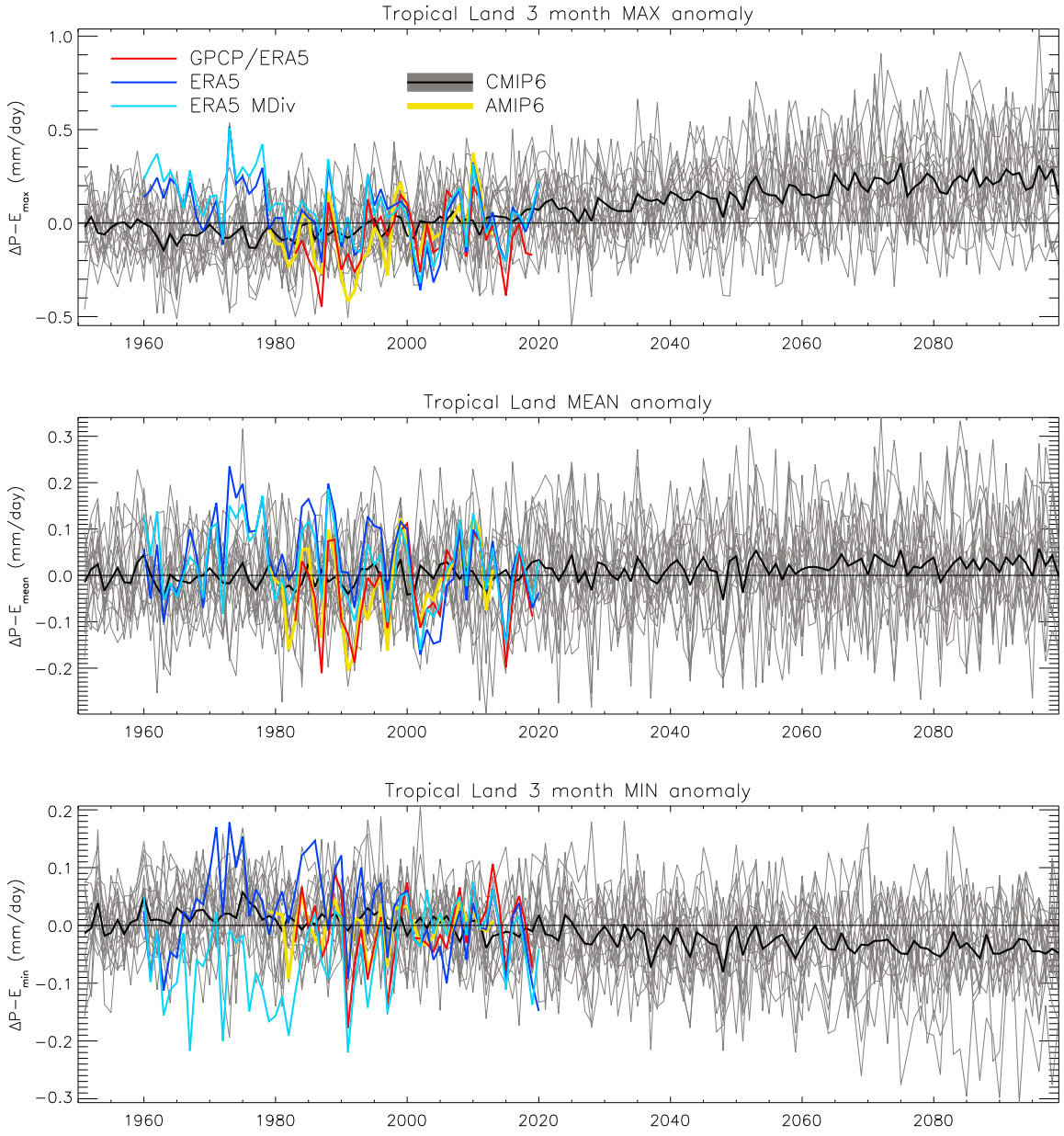

Figure S13: As Fig.4c-e but for tropical land P−E.

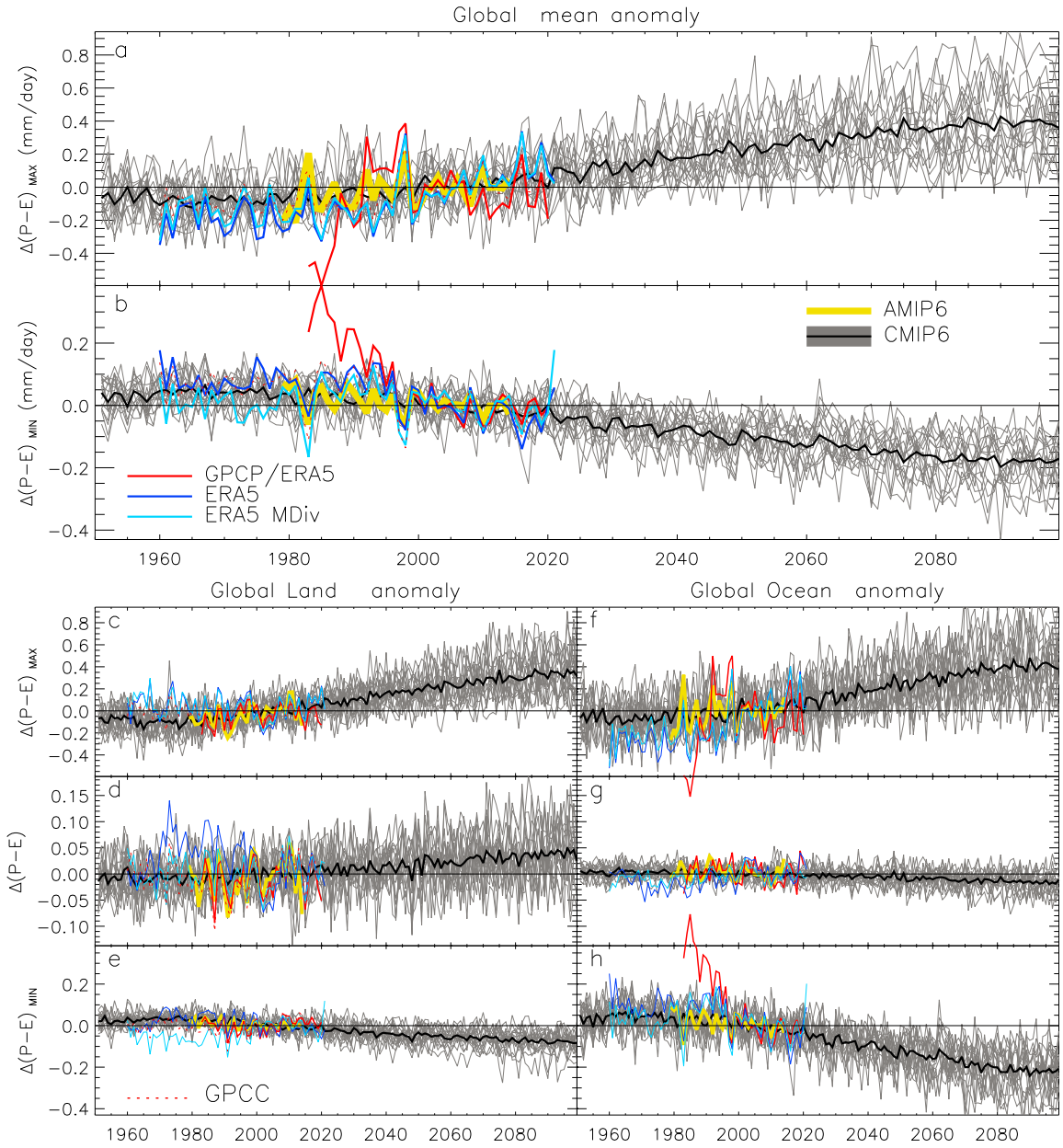

Figure S14: As Fig. 4 but for annual 1-month maximum and minimum P−E.

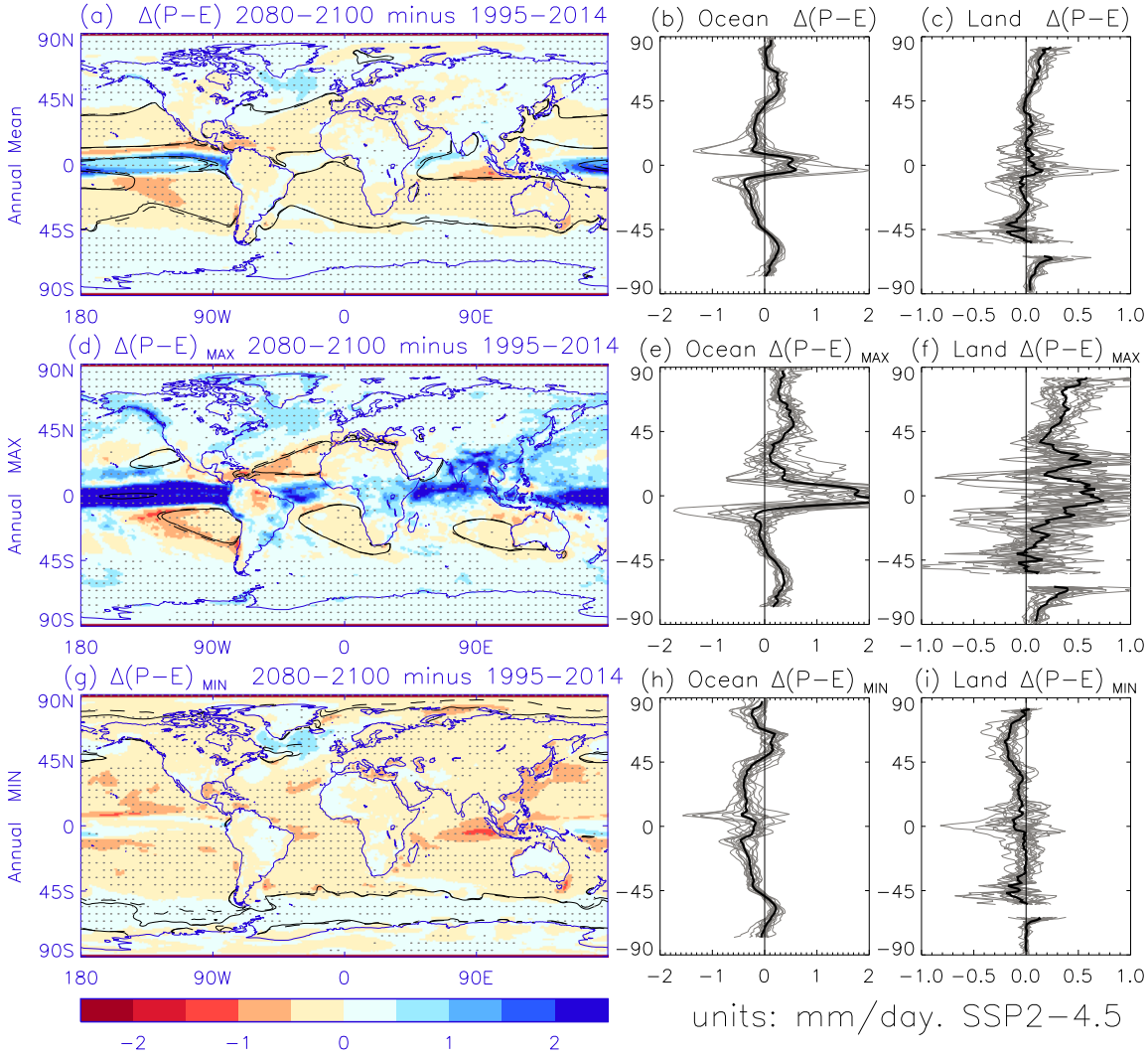

Figure S15: As Fig.5a-i but for annual 1-month maximum and minimum P−E.

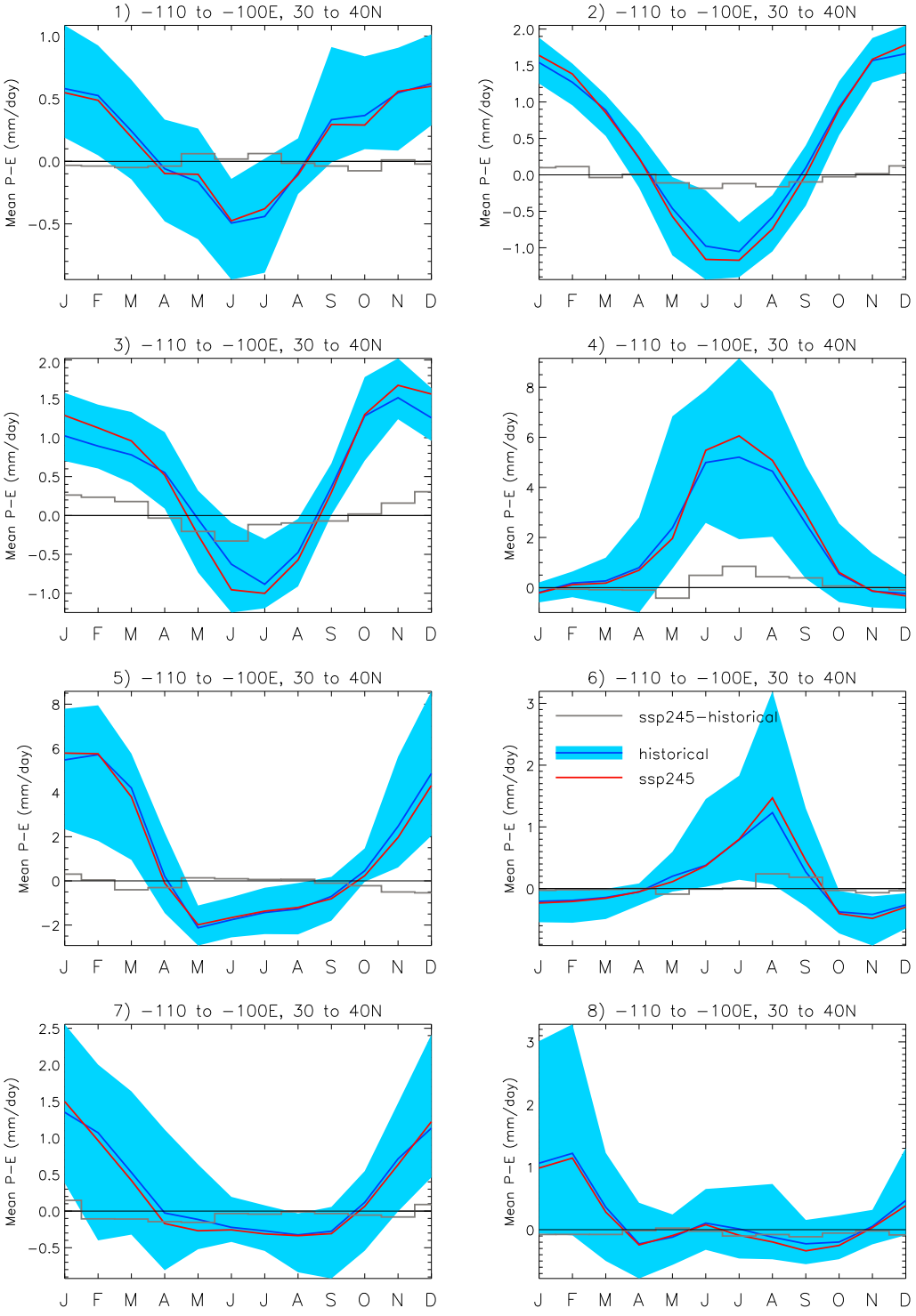

Figure S16: As Fig.1 seasonal insets (1-8) but showing CMIP6 historical (1995-2014) and ssp2-4.5 projections (2080-2100) and differences in P−E.

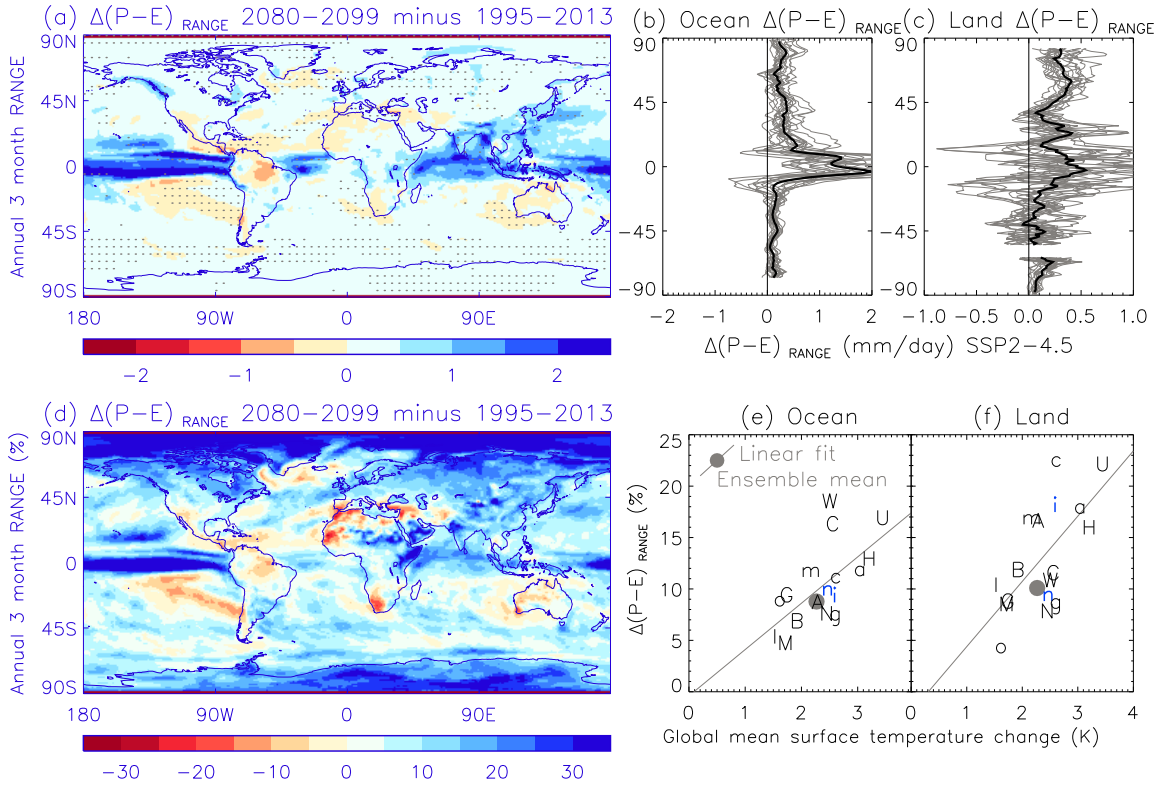

Figure S17: Projected change in (a) P−E annual 3-month maximum minus minimum range in *mm/day* (2080-2100 minus 1995-2013) and for zonal means over ocean (b) and land (c). Percentage changes in P−E range (d) and mean changes in P−E range as a percentage of present day over global (e) ocean and (f) land across models.